Research Square

Preprints are preliminary reports that have not undergone peer review.
They should not be considered conclusive, used to inform clinical practice,
or referenced by the media as validated information.

Multi-omics analysis reveals molecular mechanism of flavonol biosynthesis during the formation of petal color in Camellia nitidissima

Yi Feng
Research Institute of Subtropical Forestry Chinese Academy of Forestry
Jiyuan Li
Research Institute of Subtropical Forestry Chinese Academy of Forestry
Hengfu Yin
Research Institute of Subtropical Forestry Chinese Academy of Forestry
Jian Shen
Jinhua Forestry Technology Promotion Station of Zhejiang Province
Weixin Liu
lwx060624@163.com

Research Institute of Subtropical Forestry Chinese Academy of Forestry

Research Article

Keywords: Camellia nitidissima, Flavonol, Multi-omics analysis, CnFLS2, Jasmonate

Posted Date: May 7th, 2024

DOI: https://doi.org/10.21203/rs.3.rs-4326929/v1

License: This work is licensed under a Creative Commons Attribution 4.0 International License.
Read Full License

Additional Declarations: No competing interests reported.

Abstract

Background

Camellia nitidissima is a rare and prized species of camellia with golden-yellow flowers, and has high ornamental, medicinal and economic value. Previous studies showed that the content of flavonol accumulated greatly in petals during the formation of golden petal. However, the molecular mechanism of golden flower formation in *C. nitidissima* remains largely unknown.

Results

In this study, we performed an integrative analysis of transcriptome, proteome, and metabolome of petals at five developmental stages to construct the regulatory network during golden flower formation in *C. nitidissima*. Metabolome analysis showed that 323 flavonoids were detected, and epically two flavonols, the quercetin and kaempferol glycosides, were highly accumulated in the golden petals. And transcriptome and proteome sequencing suggested that the expression of flavonol biosynthesis genes or proteins was increased in golden petal stage, whereas expression of anthocyanin and proanthocyanidin genes or proteins were decreased. Further investigation revealed that several putative transcription factors, *MYB*s and *bHLHs*, were identified as potentially involved in flavonoid biosynthesis. Expression analysis showed that *Flavonol Synthase gene 2* (*CnFLS2*) was specifically overexpressed in petals, and the expression of *CnFLS2* of petals at five developmental stages was positively correlated with flavonol content. Overexpression of *CnFLS2* in petals increased flavonol content. Furthermore, analysis showed that the jasmonate (JA) pathways was positively correlated with flavonol biosynthesis, and methyl jasmonate (MeJA) treatment induced the expression of *CnFLS2* and the accumulation of flavonol.

Conclusions

This work describes that JA-*CnFLS2* module regulates flavonol biosynthesis during golden petal formation in *C. nitidissima*.

Background

Flavonoids are the largest pigment group in plants and the decisive factor of flower color formation in most plants [1, 2]. According to their structure, flavonoids can be classified into flavonols, anthocyanins, proanthocyanidins, flavones, isoflavones, chalcones, aurones and so on [3]. Anthocyanins can give plants red, orange, purple and blue [4]; and flavonols, chalcones and aurones are the important pale-yellow or yellow pigments in plants [5, 6]. Besides, flavonoids can be as edible pigments and taste-regulating components in food and wine [7, 8], and are also associated with health-promoting functions such as antioxidant, vasodilator, anti-carcinogenic, anti-aging activities [9, 10].

Flavonoids are synthesized through the phenylpropanoid pathway, and more than 9000 flavonoids have been identified in plants [3, 11]. Flavonols are an important branch of the flavonoid biosynthesis pathway. The biosynthesis of flavonols begins with phenylalanine, which is converted to coumaroyl-CoA through phenylalanine ammonia lyase (PAL), cinnamic acid 4-hydroxylase (C4H), and 4-coumarate: CoA ligase (4CL) [8, 12]. Dihydroflavonols, which include dihydrokaempferol (DHK), dihydroquercetin (DHQ) and dihydromyricetin (DHM), are generated from coumaroyl-CoA under the catalysis of chalcone synthase (CHS), chalcone isomerase (CHI), flavanone 3-hydroxylase (F3H), flavanone 3'-hydroxylase (F3'H), and flavanone 3'5'-hydroxylase (F3'5'H) [13–15]. Dihydroflavonols are the key intermediate metabolites in flavonoid biosynthesis and can be converted to flavonols through the activity of flavonol synthase (FLS) [16]. In addition, anthocyanin and proanthocyanidin can be generated from dihydroflavonols by dihydroflavonol 4-reductase (DFR), leucoanthocyanidin reductase (LAR), anthocyanidin synthase (ANS), anthocyanidin reductase (ANR) [17]. DFR and FLS compete with the substrate dihydroflavonol and flowe into the anthocyanin, proanthocyanidin and flavonol biosynthetic pathways, respectively [18].

In the transcriptional regulation of flavonol metabolism, MYB transcription factors and their MBW complex, composed of MYB, bHLH and WD40, are the most widely and clearly studied factors [19, 20]. In *Arabidopsis thaliana*, subgroup 7 MYB family members AtMYB11, AtMYB12 and AtMYB111 activate the expression of *CHS*, *CHI*, *F3H* and *FLS* genes, leading to increased flavonol content [21]. CsMYB60, a homologous protein of AtMYB111, activates the expression of *CsFLS* and *CsLAR* through binding to their promoters and increases the expression of *Cs4CL* and *CsCHS*, thereby promoting the biosynthesis of flavonols and proanthocyanidins in *Cucumis sativus* [22]. In addition to MYB transcription factors, hormones including jasmonate (JA), auxin, ethylene, and gibberellin (GA) are involved in the regulation of flavonol metabolism in plants. The preharvest methyl jasmonate (MeJA) treatment increased the flavonol content in red raspberry [23] and promoted anthocyanin accumulation in *Arabidopsis* [24].

The number of Camellia species and varieties has exceeded 20000, but its petal colors are mainly red, and yellow flower varieties are rare, accounting for less than 1% [25]. *Camellia nitidissima* is a rare and prized species of Genus *Camellia*, known for its unique golden flower color, honored as ‘giant panda in the plant world’ and ‘the queen of camellias’, and listed as a national second-class protected plant in China [26], possessing high ornamental worth and great economic value. Besides, the golden flowers of *C. nitidissima* are rich in flavonoids, especially flavonols [27–29], which have a variety of physiological activities including antioxidant, anti-aging, lipid lowering, blood pressure lowering effects and have huge economic value in medical care and food production [9, 10]. Therefore, *C. nitidissima* is a precious species integrating ornamental, medicinal and edible functions, as well as a valuable resource for molecular mechanism research of yellow flower formation and yellow camellia breeding.

Previous studies showed that flavonols were the main pigment in the golden petals of *C. nitidissima* [27, 28]. However, the molecular mechanism of flavonol biosynthesis during the formation of golden color in *C. nitidissima* petals remains largely unknown. To investigate this, we used petals of *C. nitidissima* at five different development periods as study materials and carried out combined multi-omics analyses, metabolome, transcriptome (based on full-length transcriptome), and proteome, transient transfection,

and MeJA treatment experiments to identify the potential pathways of flavonol accumulation during golden flower formation in *C. nitidissima*.

Results

Metabolome analysis of C. nitidissima petal

The phenotypic changes of petals during five developmental stages were observed (Fig. 1a). To analyze the metabolic changes of flavonoids in petals of *C. nitidissima*, we performed metabolome analysis with UPLC-MS/MS. Fifteen samples were divided into five groups with three replicates each for metabolic study. The OPLS-DA score map showed good variability among groups (Fig. 1b). Finally, a total of 323 flavonoids were screened, including 114 flavonols (35.29%), 59 tannin (18.27%), 28 flavones (8.67%), 24 flavanols (7.43%), 23 flavonoid carbonoside (7.12%), 21 flavanones (6.50%), 13 anthocyanins (4.02%), 11 isoflavones (3.41%), 10 proanthocyanidins (3.10%), 10 chalcones (3.10%), eight flavanonols (2.48%) (Fig. 1c).

Analysis of the differentially expressed metabolites (DEMs)

We conducted further analysis of the DEMs in the different five developmental stages of petals, a total of 285 DEMs were obtained. In the comparisons of S0 vs. S1, S1 vs. S2, S2 vs. S3, and S3 vs. S4, there were 147, 51, 117, and 57 DEMs (Fig. 2a), of which 109, 26, 66, and 30 were upregulated and 38, 25, 53, and 27 were downregulated, respectively (Fig. 2b). We used Pearson correlation analysis to determine the correlation of the differential metabolites and created a heat map of the correlation for the differential metabolites, the differential metabolite chord diagram is shown in Fig. 2C and Supplementary Fig. 1, correlation analysis showed good correlation between DEMs. K-means clustering analysis was performed to classify the expression patterns of DEMs, 12 sub-classes were obtained and the number ascribed to each class was also recorded (Supplementary Fig. 2). Further thermogram analysis showed that there were 97 metabolites positively related to the formation of golden flowers (Fig. 2d). These included 79 flavonols, in particular, including 40 quercetin-related glycosides and 27 kaempferol-related glycosides. There were 45 metabolites negatively related to the formation of golden flower, including eight proanthocyanidins and four anthocyanins (Fig. 2e). These results indicate that the accumulation of flavonols glycosides may be key metabolites during the formation of the golden color of *C. nitidissima*. Therefore, to explore the possible mechanism by which flavonols accumulation differences in *C. nitidissima*, we conducted transcriptome and proteome sequencing.

Transcriptome sequencing (RNA-seq) analysis

Transcriptome sequencing was performed on the same 15 samples used for metabolome analysis with an Illumina HiSeq platform. After quality filtering, a total of 112.88 Gb clean data were generated by Illumina HiSeq sequencing. The clean data of all samples was not less than 6.37 Gb, with an average of 7.53 Gb, the percentage of Q30 base was 92.39% or more, and GC content reached 44.30-44.69%

(Supplementary Table 1). A total of 122,201 unigenes were obtained after sequence assembly; the average length of a unigene was 2219 base pairs (bp), with an N50 value of 2699 bp. To annotate the functions of these unigenes, their sequences were submitted to seven functional databases (KEGG, NR, Swiss-Prot, GO, COG/KOG, Trembl, and Pfam) to search for annotations. The number of annotated unigenes in the seven databases ranged from 66,946 to 107,850, corresponding to annotation percentages of 54.78–88.26% (Supplementary Table 2). Among them, 21,920 (20.14%) unigenes showed high similarity with sequences of *Vitis vinifera*, and 4892 unigenes had good matches with genes from *Camellia sinensis*, followed by *Quercus suber* (Supplementary Fig. 3).

To validate the reproducibility and reliability of the RNA-seq data, 14 flavonoid- and hormone-related genes were selected for further qRT-PCR investigation. The expression trend obtained by qRT-PCR was consistent with that of the RNA-seq data (Supplementary Fig. 4), indicating that the RNA-seq results were trustworthy.

Differentially expressed genes (DEGs) analysis

Correlation analysis of the transcriptome samples was performed for each period, based on the expression levels of the DEGs. The results showed good reproducibility between samples (Supplementary Fig. 5). DEGs were screened out using the criteria |log2Fold Change| ≥ 1 and FDR < 0.05 thresholds. In total, 46,637 DEGs were identified using the DESeq2/ edgeR package. In the comparisons of S0 vs. S1, S1 vs. S2, S2 vs. S3, and S3 vs. S4, there were 2902, 881, 26,616, and 22,028 DEGs (Fig. 3a), of which 1234, 423, 12,833, and 12,035 were upregulated and 1668, 458, 13,783, and 9993 were downregulated, respectively (Fig. 3b). K-means clustering analysis was carried out to classify the expression patterns of DEGs, and eight sub-classes were identified (Fig. 3c). The results suggested that sub-class 6 was relevant to the flavonol accumulation in *C. nitidissima*, whereas the expression of genes in sub-classes 4 and 7 was negatively correlated with flavonol accumulation (Fig. 3c). Furthermore, KEGG enrichment analysis showed that ‘Metabolic pathways’, ‘Biosynthesis of secondary metabolites’, ‘Plant hormone signal transduction’, ‘Plant-pathogen interaction’ were the top four (Fig. 3d).

We detected many DEGs involved in the flavonoid biosynthesis pathway (Fig. 4a), including the biosynthesis genes *PAL*, *C4H*, *4CL*, *CHI*, *F3H*, *FLS*, *DFR*, and *ANS*. Many *MYB* and *bHLH* genes were obtained (Supplementary Fig. 6), of which 20 *bHLH* (Fig. 4b) and six *MYB* (Fig. 4c) genes were annotated in the flavonoid pathway. Many hormone-related genes, in particular JA, were screened (Fig. 4d). These included JA biosynthesis genes *LOXs*, *AOCs*, and *JAR1s*; JA receptor protein genes *COI1s*; JA degradation related genes *IAR3/ILL6s* and *ST2as*; and JA signaling genes *JAZs*. These results indicate that flavonoid-related, JA-related, and *MYB* and *bHLH* genes may have key roles in flavonol biosynthesis in petals of *C. nitidissima*. Network correlation analysis showed that JA-related, transcription factors (MYB and *bHLH*), and flavonoid biosynthesis genes, were closely related (Fig. 4e).

Proteome sequencing analysis

Proteome sequencing was performed on the same 15 samples used for metabolome and transcriptome analysis. A high Pearson's correlation coefficient for each group indicated that the data was reliable and

could be used for subsequent analyses (Fig. 5a). In total, 27,173 peptides were inferred, and 6642 proteins were confidently identified. The number of peptides in each sample ranged from 17,255 to 23,405, and the number of proteins reached 5319 to 6082 (Supplementary Table 3). A total of 3842 differentially expressed proteins (DEPs) were screened out using the criteria fold change ≥ 1.5, $P < 0.05$ to indicate upregulated proteins and fold change $\leq 1/1.5$, $P < 0.05$ for downregulated proteins. In the comparisons of S0 vs. S1, S1 vs. S2, S2 vs. S3, and S3 vs. S4, there were 880, 1124, 1870, and 1130 DEPs, including 538, 703, 919, and 300 upregulated DEPs and 342, 421, 951, and 830 downregulated DEPs, respectively (Fig. 5b). KEGG enrichment analysis revealed that DEPs of 'Metabolic pathways' and 'Biosynthesis of secondary metabolites' were the most abundant (Supplementary Fig. 7).

Differential protein analysis

In the analysis of proteome, many DEPs were found to participate in the flavonoid biosynthesis process, consistent with findings from the transcriptome data, including two 4CLs, one FLS, one GST, one LAR, two ANRs and seven UGTs (Fig. 5c). Moreover, many DEPs related to JA (Fig. 5d,) were detected: JA biosynthesis proteins LOXs, OPRs, AOCs; JA metabolism-related proteins ST2as. Furthermore, network correlation analysis showed that JA-related and flavonoid biosynthesis related proteins were closely related (Fig. 5e), as found in the transcriptome analysis.

Flavonoid biosynthesis pathway in petals of C. nitidissima

Based on the conjoint analysis, DEGs, DEPs and DEMs were mapped to the flavonoid biosynthesis pathway (Fig. 6). The results showed that the expression level of 15 key genes or proteins in flavonoid biosynthesis were significantly different among the five developmental stages of petals in *C. nitidissima* and that these differences coincided with the changes in flavonoid content (Fig. 6). The transcript abundance of six key structural genes including *PAL* (five DEGs), *C4H* (four DEGs), *CHI* (three DEGs), *F3H* (one DEGs), *F3'H* (three DEGs) and *F3'5'H* (two DEGs) genes were higher in S3-S4 (golden petal) stages than other stages, consistent with the high abundance of flavonols and petal color change in these stages. For 4CL, four DEGs and two DEPs were detected, and their expression was consistent with the change in flavonol accumulation. For FLS, the key enzyme in the flavonol biosynthesis, there were seven DEGs and one DEP identified in the conjoint analysis. UGT (seven DEGs and two DEPs) catalyzes glycosylation of flavonol, and GST (eight DEGs and one DEP), the transporter of flavonoid, might be responsible for transferring flavonol-glycosides to vacuoles.

In the biosynthetic steps from dihydroflavonols (DHK, DHQ and DHM) to anthocyanins and proanthocyanidins, the expression of DFR (nine DEGs), ANS (three DEGs), LAR (three DEGs and one DEP), ANR (eight DEGs and two DEPs), and UGTs (four DEGs and five DEPs) showed a downward trend. This was contrary to the expression of FLS and flavonol accumulation but consistent with the biosynthesis of anthocyanins and proanthocyanidins.

JA may be involved in the regulation of flavonol biosynthesis

As shown in Fig. 7, the expression of JA biosynthesis genes LOX, AOC, OPR was higher in late stages (S3 and/or S4) than in the early stages (S0, S1, S2). Second, the expression of IAR3/ILL6 and ST2a, which degraded JA-Ile and then reduced JA signaling, was highly expressed in early stages, and the JA receptor protein COI1 was upregulated in S3 and/or S4. Finally, the expression of *JAZ* (12 DEGs), the core regulator of JA signaling, showed a downward trend, which was contrary to that of biosynthesis and receptor genes. These results suggest that JA is positively correlated with flavonol biosynthesis in *C. nitidissima*.

JA and CnFLS2 regulate flavonol biosynthesis

FLS is the key and rate-limiting enzyme in the flavonol biosynthesis pathway (Liu et al., 2021). We found multiple *FLS* transcripts in the transcriptome analysis, and sequence alignment found that there were four *FLS* genes in *C. nitidissima*, named *CnFLS1*, *CnFLS2*, *CnFLS3*, and *CnFLS4* (Supplementary Fig. 8). Tissue-specific analysis showed that only *CnFLS2* was highly expressed in petals (Fig. 8b), and *CnFLS1* and *CnFLS4* were specifically highly expressed in leaves and stamens (Fig. 8a, d), while *CnFLS3* had the highest expression level in pistils (Fig. 8c). Based on transcriptome and metabolome data, the expression of *CnFLS2* of petals at five developmental stages was positively correlated with flavonol content (Fig. 8e, f).

We constructed an overexpression vector for the *CnFLS2* gene to perform the transformation in *C. nitidissima* petals through Agrobacterium -mediated transient transformation. Overexpression of *CnFLS2* in petals significantly increased *CnFLS2* expression (Fig. 8g) while promoting flavonol accumulation (Fig. 8h). The results suggest that the *FLS* gene family member *CnFLS2* may be the key gene for flavonol synthesis of petals in *C. nitidissima*.

The results of the conjoint analysis of DEMs, DEGs, and DEPs indicated that the JA pathways had strong correlations with flavonol biosynthesis (Fig. 9a). Correlation analysis of transcriptome (Fig. 4e) showed that *CnFLS2* was strongly correlated with 16 JA-related transcripts. Among them, there were strongly positively correlated with JA biosynthesis and receptor genes *LOX*, *JAR1*, and *COI1*, and negatively correlated with JA signaling and degradation related genes *JAZ* and *ST2a* (Fig. 4e). And correlation analysis of proteomic (Fig. 5e) showed a strong positive correlation between FLS2 protein (A0A4S4EHX4) and two proteins of LOX (A0A4S4EJA8, A0A4S4EU90).

To further explore the relationship between the flavonols, FLS2 and the JA pathway, we further treated the petals of *C. nitidissima* with exogenous JA, and found that exogenous methyl jasmonate (MeJA) treatment induced the expression of *CnFLS2* (Fig. 9b) and the accumulation of flavonol (Fig. 9c) in petals. The results suggest that the JA may regulate expression of *CnFLS2* to affect flavonol synthesis in petals of *C. nitidissima*.

Discussion

Flavonol biosynthesis during golden petal formation in C. nitidissima

Flower color is a key ornamental trait of ornamental plants and an important evaluation indicator of the quality and value of flowers. Camellia varieties with yellow flowers are scarce [28], and *C. nitidissima* is a rare and prized species with golden-yellow flowers in camellia, suggesting that it is a valuable resource for molecular mechanism research of yellow flower formation and yellow camellia breeding. In this study, we conducted a flavonoid metabolome analysis of five periods-based changes in petal color in *C. nitidissima* (Fig. 1a). A total of 323 flavonoid metabolites were detected, among which flavonol was the most abundant (114 metabolites), accounted for 35.29% (Fig. 1c). Compared with other Camellia plants, the golden petals of *C. nitidissima* show more accumulation of flavonol glycosides, including Quercetin-7-O-glucoside, quercetin-3-O-glucoside, quercetin-3-O-rutinoside [27, 28]. Here, we detected 79 flavonol glycosides, in particular, quercetin-related glycosides and kaempferol-related glycosides (Fig. 2d), that were positively correlated with golden petal formation. These results suggested that the glycosides of quercetin and kaempferol are the main flavonoids metabolites in the golden petals of *C. nitidissima*.

The biosynthetic pathway of plant flavonoids has been elucidated [3, 8, 33]. The expression of flavonoid structural genes, such as *PAL*, *CHI*, *CHS*, *FLS*, *DFR*, *ANS*, *LAR*, and *ANR* produces various flavonoid metabolites, including flavonols, anthocyanins and proanthocyanidins [34–36]. In this study, transcriptome and proteome sequencing were implemented to explore the regulatory pathways of flavonol accumulation. First, the flavonol biosynthesis genes *PAL*, *C4H*, *4CL*, *CHI*, *F3H*, *F3'H*, *F3'5'H*, *UGT*, *GST*, and *FLS*, were found to be highly expressed in the golden petal phase (Fig. 6), consistent with the accumulation of flavonol glycosides. Second, the expression of anthocyanin and proanthocyanidin biosynthesis genes *DFR*, *ANS*, *UGT*, *LAR*, *ANR* showed a downward trend during petal development (Fig. 6). *FLS* and *DFR* are key structural genes by which flavonoids enter different synthetic branches [3, 37, 38]. Studies have also shown that DFR and FLS competed for common dihydroflavonol substrates, and their expression inhibits each other's transcription [16, 39]. Heterologous expression of *Rosa rugosa RrDFR1* and *Petunia hybrida PhDFR* in tobacco has been reported to inhibit the expression of the endogenous *NtFLS* and promote the biosynthesis of anthocyanins [18]. In this study, during the early development stage (S0-S2) of *C. nitidissima*, *DRF* was highly expressed, and flavonoids entered the anthocyanins and proanthocyanidins branching pathway. When petals entered the golden stage (S3-S4), expression of *DFR* was downregulated, and *FLS* was highly expressed, and flavonols were synthesized. In addition, the expression of proteins 4CL, FLS, GST, LAR, ANR and UGT was consistent with their gene's expression and with flavonols biosynthesis in *C. nitidissima*. Thus, the upregulated expression of flavonol-related genes and proteins, especially FLS, and the downregulated expression of anthocyanin and proanthocyanidin genes lead to massive biosynthesis of flavonol glycosides in the process of golden color formation.

MYB and bHLH transcription factors are the vital transcription regulator of flavonoid metabolism [40–42]. GtMYBP3 and GtMYBP4 regulate genes involved in early biosynthesis of flavonoids and promote flavonol biosynthesis [43]. The bHLH transcription factor AcB2 has been shown to interact with AcMYB1 and increase anthocyanin biosynthesis in onion [44]. After our KEGG analysis, there were 20 *bHLH* and six *MYB* genes annotated into the flavonoid pathway (Fig. 4b, c). Furthermore, network correlation analysis showed that 16 *bHLH* and five *MYB* genes were closely related to flavonoids, hormone genes,

and flavonoid metabolites (Fig. 4e), indicating that these *bHLH* and *MYB* genes might be key regulators of flavonoid pathway in *C. nitidissima*.

CnFLS2 may be the key gene of flavonol biosynthesis during golden petal formation in C. nitidissima

FLS is the key structural and rate-limiting genes of flavonol biosynthesis in plants [3]. Overexpression of *FLS* increases the biosynthesis of flavonols [45, 46]. Three *FLS* genes, *CsFLSa/b/c*, exist in tea plant (*Camellia sinensis*); and heterologous overexpression of *CsFLSa/b/c* in tobacco can promote the accumulation of flavonol and the reduction of anthocyanidin in petals [16]. There are six *FLS* gene family members in *A. thaliana*, and overexpression of *AtFLS1* makes its seed coat color light brown, while *fls1-3* mutant accumulates more anthocyanidin [47]. In our *C. nitidissima*, we found four *FLS* gene (*CnFLS1/2/3/4*) members (Supplementary Fig. 8). And only *CnFLS2* was specifically overexpressed in petals (Fig. 8b), and the expression trend of *CnFLS2* during petal development was positively correlated with flavonol content (Fig. 8e, f). The results imply that the *FLS* gene family member *CnFLS2* may be a key gene in the flavonol biosynthesis of petals in *C. nitidissima*. And instantaneous expression of *CnFLS2* in petals promoted the expression of *CnFLS2* (Fig. 8g) and increased the content of flavonol (Fig. 8h). The results further suggest that *CnFLS2* may be the key gene for flavonol synthesis of petals in *C. nitidissima*.

JA may be involved in the regulation of flavonol biosynthesis during golden petal formation

Hormones are crucial for the processes of plant growth and development, including flavonoid metabolism [33, 48]. Such hormones include auxin [49], JA [50], GA [51], BR [52], strigolactone [53], ethylene [54]and abscisic acid [55]. JA positively regulates biosynthesis of various flavonoids, including anthocyanins [56], proanthocyanidins [57, 58], flavonols, and flavones [59]. Here, we detected many JA biosynthesis and signaling genes (Fig. 4d) or proteins (Fig. 5d) in *C. nitidissima*. MeJA was shown to promote the flavonol biosynthetic enzyme genes *FLS*, *F3H*, *CHS*, and *CHI* and transcription factor *MYB81* in *Gynostemma pentaphyllum* [60]. In our *C. nitidissima*, the expression trend of JA biosynthesis genes (Fig. 4d) was consistent with the trend of flavonol synthesis genes (Fig. 4a) and flavonol content (Fig. 2d), with high expression in golden petal stage, while the negative regulation genes of JA pathway were opposite. Furthermore, network correlation analysis showed that the genes and proteins of JA pathways were strong correlations with flavonol biosynthesis genes and proteins and flavonol metabolites (Fig. 9a). The results indicated that JA might positively regulate flavonol biosynthesis in petals of *C. nitidissima*. MeJA treatments increased the content of flavonols such as myricetin and quercetin and the activity of PAL enzyme [23]. In this study, MeJA treatments promoted the expression of *CnFLS2* (Fig. 9b) and increased the content of flavonol (Fig. 9c). The results suggested that JA-*CnFLS2* module regulated flavonol biosynthesis in petals of *C. nitidissima*. However, how JA regulates the expression of *CnFLS2* and flavonol biosynthesis; this requires further study.

Conclusion

This study provides insight into the regulatory mechanism of flavonol biosynthesis in petals of *C. nitidissima* by an integrative analysis of the transcriptome, proteome, and metabolome. A total of 323 flavonoids were detected during the five developmental stages of petals, among which flavonol was the most abundant (114 metabolites), accounted for 35.29%, and epically quercetin and kaempferol glycosides were highly expressed in the golden petals. And transcriptome and proteome sequencing suggested that the expression of flavonol biosynthesis genes or proteins was increased in golden petal stage. Correlation analysis showed that the expression of *CnFLS2* of petals at five developmental stages was positively correlated with flavonol content. And Overexpression of *CnFLS2* in petals increased flavonol content. Furthermore, analysis suggested that the JA pathways was positively correlated with flavonol biosynthesis, and MeJA treatment induced the expression of *CnFLS2* and the accumulation of flavonol.

Materials and methods

Plant materials

The *C. nitidissima* plants were from the Camellia Germplasm Resources of Institute of Subtropical Forestry, Chinese Academy of Forestry (Qianjia village, Hangzhou city, Zhejiang province), where they have been grown in the field, and were about 15 years old. Petals were collected at five different developmental stages in February 2021, early-bud stage (S0), mid-bud stage (S1), late-bud stage (S2), half-opening stage (S3), and complete-opening stage (S4), then immediately frozen in liquid nitrogen, and stored at -80°C for subsequent analysis.

Metabolic analysis

Biological samples are freeze-dried and dissolve 100mg of lyophilized powder with 1.2ml 70% methanol solution, the extracts were filtrated (SCAA-104, 0.22μm pore size; ANPEL, Shanghai, China, http://www.anpel.com.cn/) before UPLC-MS/MS analysis. The metabolites were qualitatively quantified by ultra-performance liquid chromatography (UPLC)-electrospray ionization (ESI)-tandem mass spectrometry (MS/MS). The analytical conditions were as follows, UPLC: column, Agilent SB-C18 (1.8 μm, 2.1 mm*100 mm); The mobile phase was consisted of solvent A, pure water with 0.1% formic acid, and solvent B, acetonitrile with 0.1% formic acid. Sample measurements were performed with a gradient program that employed the starting conditions of 95% A, 5% B. Within 9min, a linear gradient to 5% A, 95% B was programmed, and a composition of 5% A, 95% B was kept for 1min. Subsequently, a composition of 95% A, and 5.0% B was adjusted within 1.10 min and kept for 2.9 min.

Qualitative analysis of metabolites was performed based on the self-built database MWDB (Metware Biotechnology Co., Ltd. Wuhan, China) and secondary spectral information. Metabolite quantification was accomplished by multiple reaction monitoring analysis using triple four-stage MS. Unsupervised PCA and OPLS-DA (partial least squares discriminant analysis) were used to analyze metabolites.

Significantly regulated metabolites between groups were determined by VIP ≥ 1. A fold change ≥ 2 or fold change ≤ 0.5 based on the OPLS-DA results were the criteria for identification of significantly differential metabolites. Hierarchical clustering analysis of the metabolites in different samples was performed using R software (www.r-project.org/). The significantly differential metabolites were subsequently subjected to KEGG (Kyoto Encyclopedia of Genes and Genomes) analysis.

RNA sequencing (RNA-seq) analysis

Total RNA was extracted from the flowers of *C. nitidissima* using an RNA Prep Pure kit for plants (Tiangen, Beijing, China). A total amount of 1 μg RNA per sample was used as input material for RNA sample preparation. The clustering of the index-coded samples was performed on a cBot Cluster Generation System using TruSeq PE Cluster Kit v3-cBot-HS (Illumina). After cluster generation, the library preparations were sequenced on an Illumina HiSeq platform.

Use fastp v 0.19.3 to filter the original data, when any sequencing reads When the number of low-quality(Q < = 20) bases contained in reads exceeds 50% of the bases of the reads, these paired reads will be removed. Transcriptome assembly was performed using Trinity (v2.11.0). Use TransDecoder to identify candidate coding regions within transcript sequences generated by de novo RNA-Seq transcript assembly using Trinity. Gene expression levels were estimated by RSEM [30], and the expression abundance of the corresponding unigenes was calculated by the Fragments per Kilobase of Transcriptome per Million Mapped Reads method. Gene function was annotated based on the following databases: KEGG; KOG/COG (COG: Clusters of Orthologous Groups of Proteins; KOG: euKaryotic Ortholog Groups); GO (Gene Ontology); Nr (NCBI non-redundant protein sequences); Trembl (a variety of new documentation files and the creation of TrEMBL).

DESeq2 [31] was used to analyze differential expression between two groups. P-values were corrected using Benjamini and Hochberg's method. The false discovery rate (FDR) was corrected using the posterior probability values; FDR < 0.05 and $|\log_2(\text{foldchange})| \geq 1$ were regarded as the thresholds for significant differential expression.

Protein sample preparation and MS detection and data analysis

Protein in solution was precipitated using acetone, and the ground flower tissue was mixed with four volumes of lysis buffer (8 M urea, 100 mM Tris-Cl, 10 mM dithiothreitol) and incubated at 37°C for 1 h. Subsequently, 40 mM iodoacetamide was added to the complex solution. The Bradford method was used to determine protein concentration. After protein quantification, 50-μg samples were separated by sodium dodecyl sulfate polyacrylamide gel electrophoresis, and the protein bands were stained with Kemas Brilliant Blue. The extracted proteins were reduced and alkylated and then digested with trypsin. Peptides were desalted using a Sep-Pak C18 column and vacuum dried.

The MS data were acquired using a Q Exactive HF-X mass spectrometer in tandem with an EASY-nLC1200 liquid-phase liquid chromatography system. DIA-NN software was used to establish a spectrum

library based on the protein sequence database of *Camellia sinensis* var. *sinensis* in the UniProt database; protein identification was performed, and quantitative information was extracted. The test results were screened using a threshold of 1% FDR. The quantification intensity information obtained from DIA analysis was used for difference comparison, with t-test analysis after log2 transformation, data filling (imputation algorithm in Perseus software), and data normalization: fold change ≥ 1.5, $P < 0.05$ indicated upregulated proteins, fold change ≤ 1/1.5, $P < 0.05$ indicated downregulated proteins.

Interaction network analysis

An interaction network was established based on Pearson's correlation coefficients, which were calculated in the R environment (https://www.r-project.org/); correlations with a coefficient of $R \geq 0.8$ or $R \leq -0.8$ and $P \leq 0.05$ were retained. The relationships between candidate genes, including transcription factors (TF) genes and structural genes, proteins, and flavonoid components were visualized using Cytoscape (v. 3.9.2).

Quantitative real-time PCR (qRT-PCR) analysis

All gene-specific primers were designed using NCBI online. The same RNA samples used in RNA-Seq were used in RT-qPCR. Each RNA sample was biologically repeated three times. *CnGAPDH* was used as the internal normalization gene (Supplementary Table 4) and relative gene expression levels were analyzed according to the $2^{\Delta\Delta Ct}$ method. The qRT-PCR was carried out as described previously [28].

Transient overexpression of CnFLS2 in C. nitidissima

Take branches with flowers and cultivate them in water for 1 day. The petals of complete-opening stage were used for transient overexpression using agrobacterium-mediated transformation system. Transfer of target vector (pCAMBIA1302-CnFLS2 and pCAMBIA1302) into agrobacterium strain GV3101, shake the agrobacterium to around 0.8 OD600 and centrifugation at 5,000 rpm for 8 min. Resuspended precipitates with infiltration buffer (10 mM MES, 10 mM MgCl2, 100 uM acetosyringone, pH 5.7–5.8), and injected into petals of *C. nitidissima*. Then, the branches were cultivated at 24°C in the dark for 24h and maintained under 16 h-light/8 h-dark and 24°C and 50% humidity (100 mmol m^{-2} s^{-1} with fluorescent lamps) for 48 h-50 h. The petals were collected and frozen in liquid nitrogen for later analysis.

Methyl jasmonate (MeJA) treatment

The branches with flowers were used for MeJA treatment. Exogenous MeJA treatment was carried out as described previously [32]. Petals were treated with 250 μmol/L methyl jasmonate (MeJA), the control groups were treated with H_2O, the solution was dissolved in 1% ethanol. These solutions contained 0.01% Tween-20 to promote absorption. Sampled at 3H, 6H, 12H, 24H, 48H respectively and frozen in liquid nitrogen for later analysis.

Statistical analysis

Statistical analyses were carried out using SPSS (v25) software (SPSS Inc., Chicago, IL, USA). All experiments were repeated with at least three biological replicates and analyzed statistically using Student's t-test (*P < 0.05, **P < 0.01). Error bars represent the ± SE.

Declarations

Acknowledgments

Not applicable.

Author contributions

Yi Feng: Investigation, Formal Analysis, Writing—original draft. **Jiyuan Li**: Funding acquisition, Formal analysis. **Hengfu Yin**: Writing—review and editing. **Jian Shen**: Funding acquisition, Writing—review and editing. **Weixin Liu**: Conceptualization, Formal Analysis, Funding acquisition, Writing—review and editing. All the authors reviewed and approved the final manuscript. All authors have read and agreed to the published version of the manuscript.

Funding

This work was funded by National Natural Science Foundation of China (32371842), Zhejiang Provincial Natural Science Foundation of China (LQ23C150005), and Fundamental Research Funds of CAF (CAFYBB2023MB005).

Data availability statement

All data generated or analyzed during this study are included in this published article (and its supplementary information files). The sequenced raw reads generated in this study have been submitted to the National Center for Biotechnology Information (NCBI) with BioProject ID: PRJNA909942.

Ethics approval and consent to participate

Not applicable.

Consent for publication

Not applicable.

Competing interests

The authors declare no competing interests

References

1. Noda N: Recent advances in the research and development of blue flowers. *Breeding science* 2018, 68(1):79-87.
2. Zhao L, Sun J, Cai Y, Yang Q, Zhang Y, Ogutu CO, Liu J, Zhao Y, Wang F, He H *et al*: *PpHYH* is responsible for light-induced anthocyanin accumulation in fruit peel of *Prunus persica*. *Tree physiology* 2022, 42(8):1662-1677.
3. Liu W, Feng Y, Yu S, Fan Z, Li X, Li J, Yin H: The Flavonoid Biosynthesis Network in Plants. *International Journal of Molecular Sciences* 2021, 22:12824.
4. Zhang Y, Butelli E, Martin C: Engineering anthocyanin biosynthesis in plants. *Current opinion in plant biology* 2014, 19:81-90.
5. Hoshino A, Mizuno T, Shimizu K, Mori S, Fukada-Tanaka S, Furukawa K, Ishiguro K, Tanaka Y, Iida S: Generation of Yellow Flowers of the Japanese Morning Glory by Engineering Its Flavonoid Biosynthetic Pathway toward Aurones. *Plant and Cell Physiology* 2019, 60(8):1871-1879.
6. Yang Y, Li B, Feng C, Wu Q, Wang Q, Li S, Yu X, Wang L: Chemical Mechanism of Flower Color Microvariation in Paeonia with Yellow Flowers. *Horticultural Plant Journal* 2020, 6(3):179-190.
7. Yang L, Dykes L, Awika JM: Thermal stability of 3-deoxyanthocyanidin pigments. *Food chemistry* 2014, 160:246-254.
8. Winkel-Shirley B: Flavonoid Biosynthesis. A Colorful Model for Genetics, Biochemistry, Cell Biology, and Biotechnology. *Plant Physiology* 2001, 126:485-493.
9. Nabavi SM, Šamec D, Tomczyk M, Milella L, Russo D, Habtemariam S, Suntar I, Rastrelli L, Daglia M, Xiao J *et al*: Flavonoid biosynthetic pathways in plants: Versatile targets for metabolic engineering. *Biotechnology advances* 2018, 38:107316.
10. Wang ZL, Wang S, Kuang Y, Hu ZM, Qiao X, Ye M: A comprehensive review on phytochemistry, pharmacology, and flavonoid biosynthesis of *Scutellaria baicalensis*. *Pharmaceutical biology* 2018, 56(1):465-484.
11. Sun C, Zhang M, Dong H, Liu W, Guo L, Wang X: A spatially-resolved approach to visualize the distribution and biosynthesis of flavones in *Scutellaria baicalensis* Georgi. *Journal of pharmaceutical and biomedical analysis* 2020, 179:113014.
12. Wohl J, Petersen M: Functional expression and characterization of cinnamic acid 4-hydroxylase from the hornwort *Anthoceros agrestis* in *Physcomitrella patens*. *Plant cell reports* 2020, 39(5):597-607.
13. Nakatsuka T, Sasaki N, Nishihara M: Transcriptional regulators of flavonoid biosynthesis and their application to flower color modification in Japanese gentians. *Plant Biotechnology* 2014, 31(5):389-399.
14. Si C, Dong W, da Silva JAT, He C, Yu Z, Zhang M, Huang L, Zhao C, Zeng D, Li C *et al*: Functional Analysis of Flavanone 3-Hydroxylase (F3H) from *Dendrobium officinale*, which Confers Abiotic Stress Tolerance. *Horticultural Plant Journal* 2022.
15. Yu S, Li J, Peng T, Ni S, Feng Y, Wang Q, Wang M, Chu X, Fan Z, Li X *et al*: Identification of Chalcone Isomerase Family Genes and Roles of *CnCHI4* in Flavonoid Metabolism in *Camellia nitidissima*.

Biomolecules 2023, 13:41.

16. Jiang X, Shi Y, Fu Z, Li WW, Lai S, Wu Y, Wang Y, Liu Y, Gao L, Xia T: Functional characterization of three flavonol synthase genes from *Camellia sinensis*: Roles in flavonol accumulation. *Plant Science* 2020, 300:110632.
17. Giampieri F, Gasparrini M, Forbes-Hernandez TY, Mazzoni L, Capocasa F, Sabbadini S, Alvarez-Suarez JM, Afrin S, Rosati C, Pandolfini T *et al*: Overexpression of the *Anthocyanidin Synthase* (*ANS*) Gene in Strawberry Enhances Antioxidant Capacity and Cytotoxic Effects on Human Hepatic Cancer Cells. *Journal of agricultural and food chemistry* 2018, 66(3):581-592.
18. Luo P, Ning G, Wang Z, Shen Y, Jin H, Li P, Huang S, Zhao J, Bao M: Disequilibrium of Flavonol Synthase and Dihydroflavonol-4-Reductase Expression Associated Tightly to White vs. Red Color Flower Formation in Plants. *Frontiers in plant science* 2016, 6:1257.
19. Xu W, Dubos C, Lepiniec L: Transcriptional control of flavonoid biosynthesis by MYB-bHLH-WDR complexes. *Trends in plant science* 2015, 20(3):176-185.
20. Zhang X, He Y, Li L, Liu H, Hong G: Involvement of the R2R3-MYB transcription factor MYB21 and its homologs in regulating flavonol accumulation in Arabidopsis stamen. *Journal of experimental botany* 2021, 72(12):4319-4332.
21. Stracke R, Ishihara H, Huep G, Barsch A, Mehrtens F, Niehaus K, Weisshaar B: Differential regulation of closely related R2R3-MYB transcription factors controls flavonol accumulation in different parts of the Arabidopsis thaliana seedling. *The Plant Journal* 2007, 50(4):660-677.
22. Li J, Luan Q, Han J, Zhang C, Liu M, Ren Z: CsMYB60 directly and indirectly activates structural genes to promote the biosynthesis of flavonols and proanthocyanidins in cucumber. *Horticulture research* 2020, 7:103.
23. Flores G, Ruiz del Castillo ML: Influence of preharvest and postharvest methyl jasmonate treatments on flavonoid content and metabolomic enzymes in red raspberry. *Postharvest Biology and Technology* 2014, 97:77-82.
24. Li T, Jia KP, Lian HL, Yang X, Li L, Yang HQ: Jasmonic acid enhancement of anthocyanin accumulation is dependent on phytochrome A signaling pathway under far-red light in *Arabidopsis*. *Biochemical and biophysical research communications* 2014, 454(1):78-83.
25. Guan K, Li J, Wang z: Camellias of China [M]. *Hangzhou: Zhejiang Science and Technology Publishing House* 2014:395-406.
26. He D, Li X, Sai X, Wang L, Li S, Xu Y: *Camellia nitidissima* C.W. Chi: a review of botany, chemistry, and pharmacology. *Phytochemistry Reviews* 2017, 17(2):327-349.
27. Tanikawa N, Kashiwabara T, Hokura A, Abe T, Shibata M, Nakayama M: A Peculiar Yellow Flower Coloration of Camellia Using Aluminum-flavonoid Interaction. *Journal of the Japanese Society for Horticultural Science* 2008, 77(4):402–407.
28. Liu W, Yu S, Feng Y, Mo R, Wang K, Fan M, Fan Z, Yin H, Li J, Li X: Comparative Transcriptome and Pigment Analyses Reveal Changes in Gene Expression Associated with Flavonol Metabolism in Yellow Camellia. *Forests* 2022, 13(7):1094.

29. Zhou X, Li J, Zhu Y, Ni S, Chen J, Feng X, Zhang Y, Li S, Zhu H, Wen Y: *De novo* Assembly of the *Camellia nitidissima* Transcriptome Reveals Key Genes of Flower Pigment Biosynthesis. *Frontiers in plant science* 2017, 8:1545.
30. Li B, Dewey CN: RSEM: accurate transcript quantification from RNA-Seq data with or without a reference genome. *BMC bioinformatics* 2011, 12:323.
31. Leng N, Dawson JA, Thomson JA, Ruotti V, Rissman AI, Smits BM, Haag JD, Gould MN, Stewart RM, Kendziorski C: EBSeq: an empirical Bayes hierarchical model for inference in RNA-seq experiments. *Bioinformatics* 2013, 29(8):1035-1043.
32. Chang L, Wu S, Tian L: Methyl jasmonate elicits distinctive hydrolyzable tannin, flavonoid, and phyto-oxylipin responses in pomegranate (*Punica granatum* L.) leaves. *Planta* 2021, 254(5):89.
33. Dong NQ, Lin HX: Contribution of phenylpropanoid metabolism to plant development and plant-environment interactions. *Journal of integrative plant biology* 2020.
34. Sasaki N, Nakayama T: Achievements and Perspectives in Biochemistry Concerning Anthocyanin Modification for Blue Flower Coloration. *Plant and Cell Physiology* 2015, 56(1):28-40.
35. Lepiniec L, Debeaujon I, Routaboul JM, Baudry A, Pourcel L, Nesi N, Caboche M: Genetics and biochemistry of seed flavonoids. *Annual Review of Plant Biology* 2006, 57:405–430.
36. Xu P, Marsafari M, Zha J, Koffas M: Microbial Coculture for Flavonoid Synthesis. *Trends in biotechnology* 2020, 38(7):686-688.
37. Kubra G, Khan M, Hussain S, Iqbal T, Muhammad J, Ali H, Gul A, Munir F, Amir R: Molecular characterization of *Leucoanthocyanidin reductase* and *Flavonol synthase* gene in *Arachis hypogaea*. *Saudi journal of biological sciences* 2021, 28(4):2301-2315.
38. Wang X, Chen X, Luo S, Ma W, Li N, Zhang W, Tikunov Y, Xuan S, Zhao J, Wang Y *et al*: Discovery of a *DFR* gene that controls anthocyanin accumulation in the spiny *Solanum* group: roles of a natural promoter variant and alternative splicing. *The Plant Journal* 2022, 111(4):1096-1109.
39. Chen W, Xiao Z, Wang Y, Wang J, Zhai R, Lin-Wang K, Espley R, Ma F, Li P: Competition between anthocyanin and kaempferol glycosides biosynthesis affects pollen tube growth and seed set of *Malus*. *Horticulture research* 2021, 8(1):173.
40. Rajput R, Naik J, Stracke R, Pandey A: Interplay between R2R3 MYB-type activators and repressors regulates proanthocyanidin biosynthesis in banana (*Musa acuminata*). *The New phytologist* 2022.
41. Sun C, Deng L, Du M, Zhao J, Chen Q, Huang T, Jiang H, Li CB, Li C: A Transcriptional Network Promotes Anthocyanin Biosynthesis in Tomato Flesh. *Molecular plant* 2020, 13(1):42-58.
42. Li C, Qiu J, Huang S, Yin J, Yang G: AaMYB3 interacts with AabHLH1 to regulate proanthocyanidin accumulation in *Anthurium andraeanum* (Hort.)-another strategy to modulate pigmentation. *Horticulture research* 2019, 6:14.
43. Nakatsuka T, Saito M, Yamada E, Fujita K, Kakizaki Y, Nishihara M: Isolation and characterization of GtMYBP3 and GtMYBP4, orthologues of R2R3-MYB transcription factors that regulate early flavonoid biosynthesis, in gentian flowers. *Journal of experimental botany* 2012, 63(18):6505-6517.

44. Li X, Cao L, Jiao B, Yang H, Ma C, Liang Y: The bHLH transcription factor AcB2 regulates anthocyanin biosynthesis in onion (*Allium cepa* L.). *Horticulture research* 2022, 2022:uhac128.
45. Yu Z, Dong W, Teixeira da Silva JA, He C, Si C, Duan J: Ectopic expression of DoFLS1 from *Dendrobium officinale* enhances flavonol accumulation and abiotic stress tolerance in *Arabidopsis thaliana*. *Protoplasma* 2021, 1.
46. Park S, Kim DH, Yang JH, Lee JY, Lim SH: Increased Flavonol Levels in Tobacco Expressing *AcFLS* Affect Flower Color and Root Growth. *International Journal of Molecular Sciences* 2020, 21(3):1011.
47. Nguyen NH, Kim JH, Kwon J, Jeong CY, Lee W, Lee D, Hong SW, Lee H: Characterization of *Arabidopsis thaliana FLAVONOL SYNTHASE 1* (*FLS1*)-overexpression plants in response to abiotic stress. *Plant Physiology and Biochemistry* 2016, 103:133-142.
48. LaFountain AM, Yuan YW: Repressors of anthocyanin biosynthesis. *The New phytologist* 2021, 231(3):933-949.
49. Wang YC, Wang N, Xu HF, Jiang SH, Fang HC, Su MY, Zhang ZY, Zhang TL, Chen XS: Auxin regulates anthocyanin biosynthesis through the Aux/IAA-ARF signaling pathway in apple. *Horticulture research* 2018, 5:59.
50. Ni J, Zhao Y, Tao R, Yin L, Gao L, Strid A, Qian M, Li J, Li Y, Shen J *et al*: Ethylene mediates the branching of the jasmonate-induced flavonoid biosynthesis pathway by suppressing anthocyanin biosynthesis in red Chinese pear fruits. *Plant Biotechnology Journal* 2020, 18(5):1223-1240.
51. Tan H, Man C, Xie Y, Yan J, Chu J, Huang J: A Crucial Role of GA-Regulated Flavonol Biosynthesis in Root Growth of *Arabidopsis*. *Molecular plant* 2019, 12(4):521-537.
52. Liang T, Shi C, Peng Y, Tan H, Xin P, Yang Y, Wang F, Li X, Chu J, Huang J *et al*: Brassinosteroid-Activated BRI1-EMS-SUPPRESSOR 1 Inhibits Flavonoid Biosynthesis and Coordinates Growth and UV-B Stress Responses in Plants. *The Plant cell* 2020, 32(10):3224-3239.
53. Wang P, Du Y, Zhao X, Miao Y, Song CP: The MPK6-ERF6-ROS-responsive cis-acting Element7/GCC box complex modulates oxidative gene transcription and the oxidative response in Arabidopsis. *Plant Physiology* 2013, 161(3):1392-1408.
54. Ma H, Yang T, Li Y, Zhang J, Wu T, Song T, Yao Y, Tian J: The long noncoding RNA MdLNC499 bridges MdWRKY1 and MdERF109 function to regulate early-stage light-induced anthocyanin accumulation in apple fruit. *The Plant cell* 2021, 33(10):3309-3330.
55. Ramegowda V, Basu S, Krishnan A, Pereira A: Rice *GROWTH UNDER DROUGHT KINASE* is required for drought tolerance and grain yield under normal and drought stress conditions. *Plant Physiology* 2014, 166(3):1634-1645.
56. Premathilake AT, Ni J, Shen J, Bai S, Teng Y: Transcriptome analysis provides new insights into the transcriptional regulation of methyl jasmonate-induced flavonoid biosynthesis in pear calli. *BMC plant biology* 2020, 20(1):388.
57. Zhu J, Yan X, Liu S, Xia X, An Y, Xu Q, Zhao S, Liu L, Guo R, Zhang Z *et al*: Alternative splicing of CsJAZ1 negatively regulates flavan-3-ol biosynthesis in tea plants. *The Plant Journal* 2022, 110(1):243-261.

58. An JP, Xu RR, Liu X, Zhang JC, Wang XF, You CX, Hao YJ: Jasmonate induces biosynthesis of anthocyanin and proanthocyanidin in apple by mediating the JAZ1-TRB1-MYB9 complex. *The Plant Journal* 2021:15245.
59. He B, Zhang Y, Wang L, Guo D, Jia X, Wu J, Qi S, Wu H, Gao Y, Guo M: Both Two *CtACO3* Transcripts Promoting the Accumulation of the Flavonoid Profiles in Overexpressed Transgenic Safflower. *Frontiers in plant science* 2022, 13:833811.
60. Huang D, Ming R, Xu S, Yao S, Li L, Huang R, Tan Y: Genome-Wide Identification of R2R3-MYB Transcription Factors: Discovery of a "Dual-Function" Regulator of Gypenoside and Flavonol Biosynthesis in *Gynostemma pentaphyllum*. *Frontiers in plant science* 2022, 12:796248.

Figures

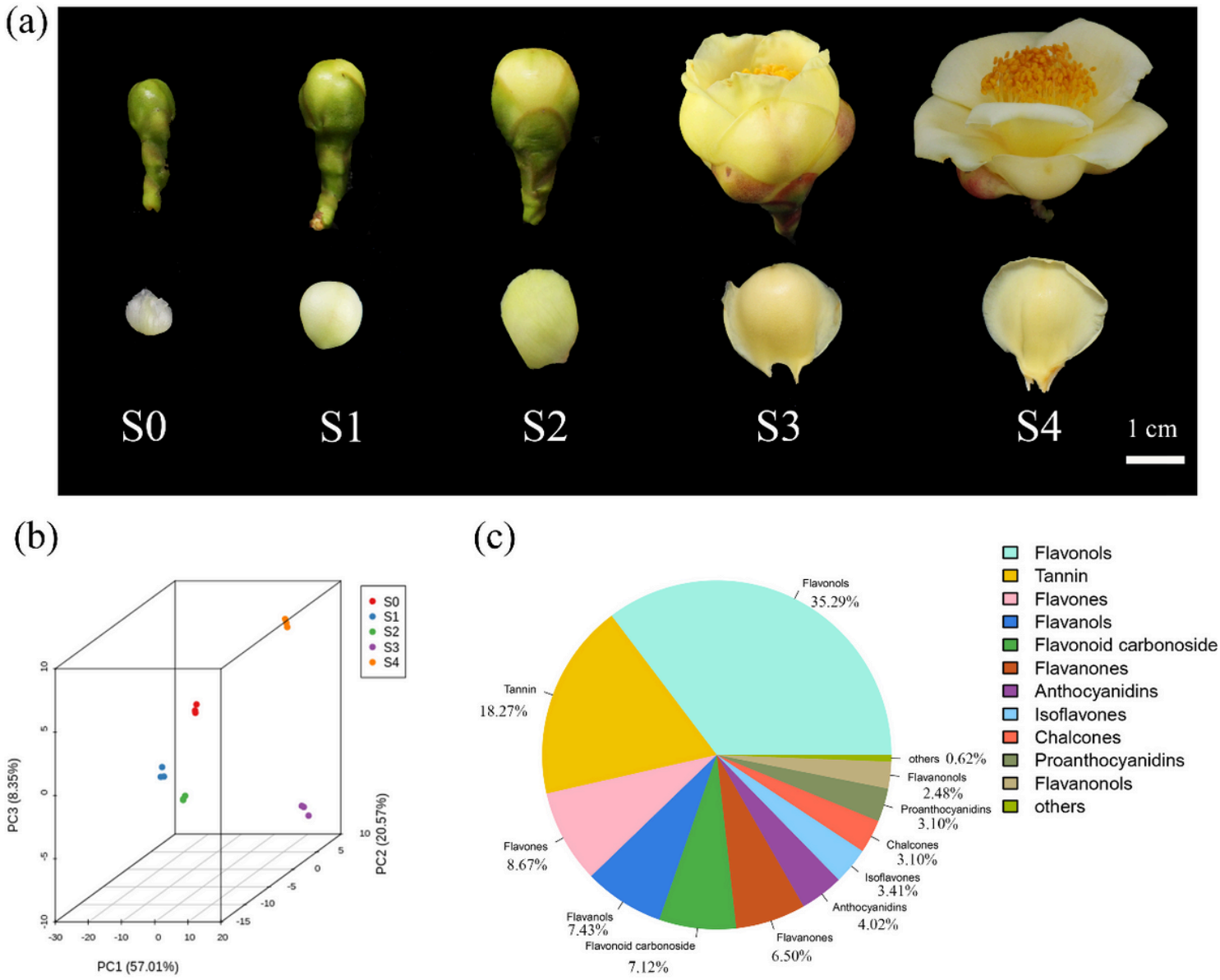

Figure 1

Petals development and metabolome analysis. (a) Five developmental stages of petals in *C. nitidissima*. S0, early-bud stage; S1, mid-bud stage; S2, late-bud stage; S3, half-opening stage; S4, complete-opening stage.(b) OPLS-DA Score Map. Each point in the graph indicates a sample, and samples of the same group are represented with the same color. (c) Number of differential metabolites.

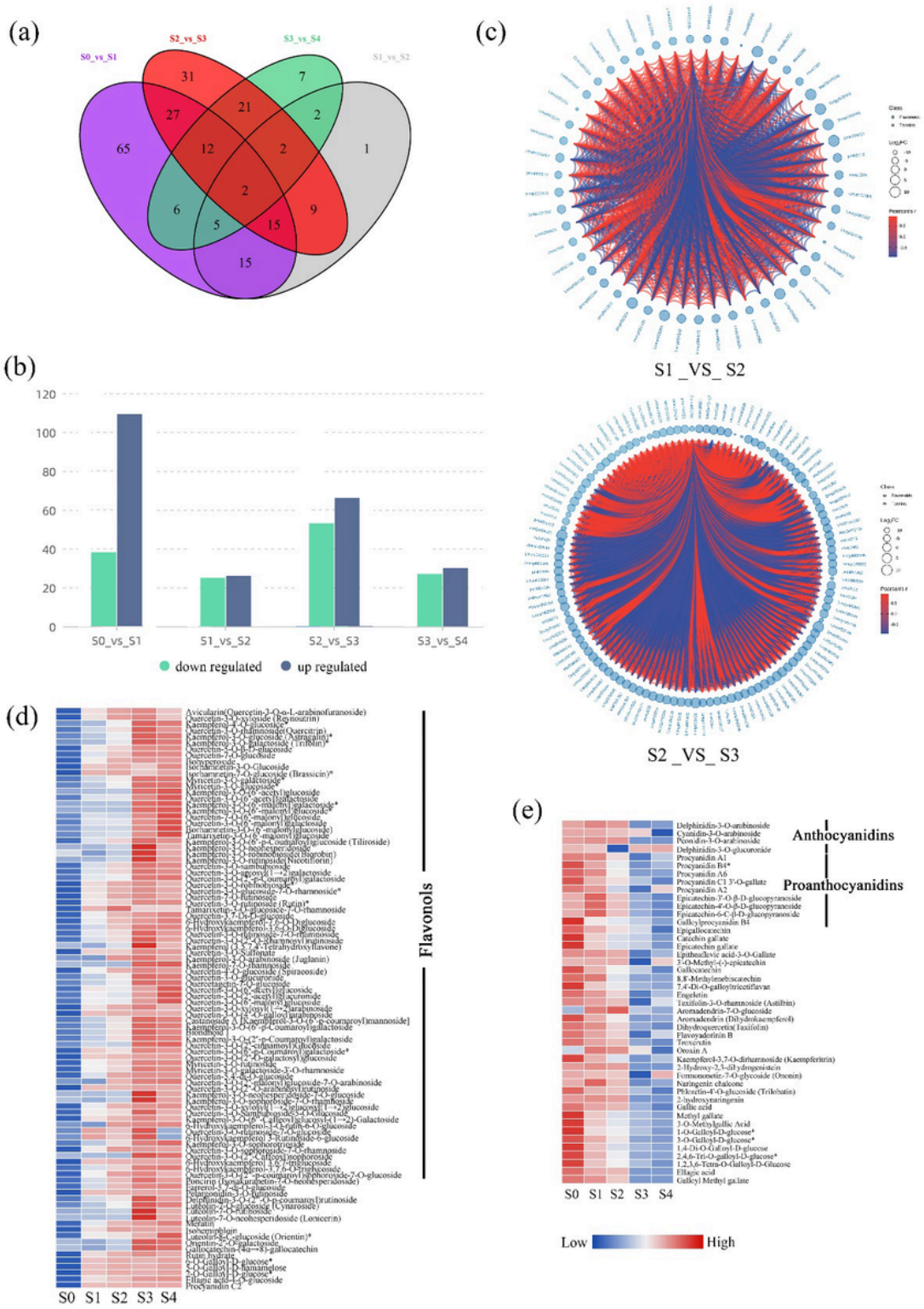

Figure 2

Differentially expressed metabolites (DEMs) analysis. (a) Venn diagram between comparisons. (b) Up- and downregulated unigenes in different comparisons. (c) The Pearson correlation analysis between comparisons. The red line represents positive correlation, and the blue line represents negative correlation. Heat maps of positively (d) and negatively (e) correlated metabolites during the formation of golden flowers.

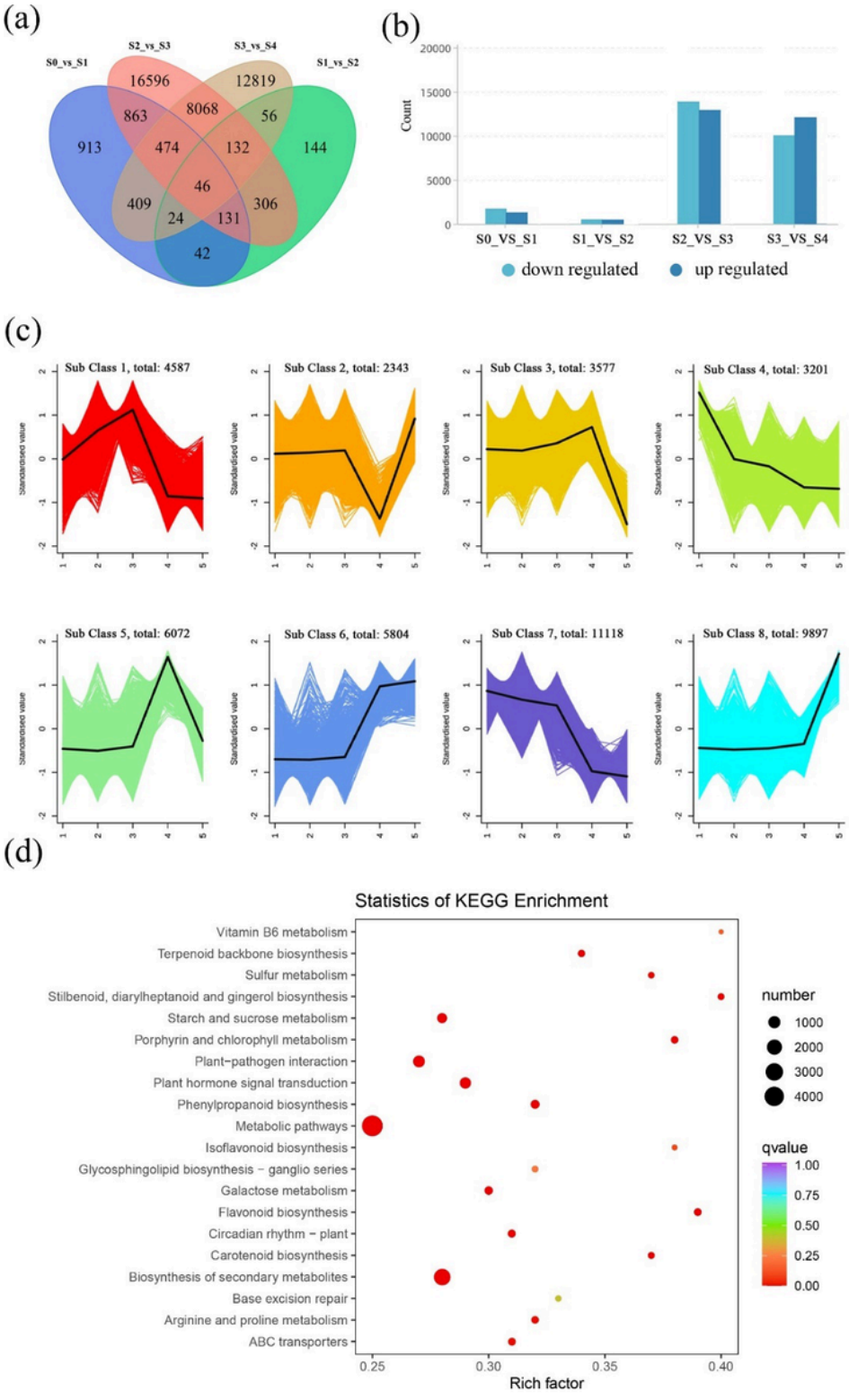

Figure 3

Transcriptome data analysis. (a) Venn diagram between comparisons. (b) Up- and downregulated unigenes in different comparisons. (c) Expression trends of the identified DEGs in five developmental stages. (d) KEGG enrichment analysis of DEGs.

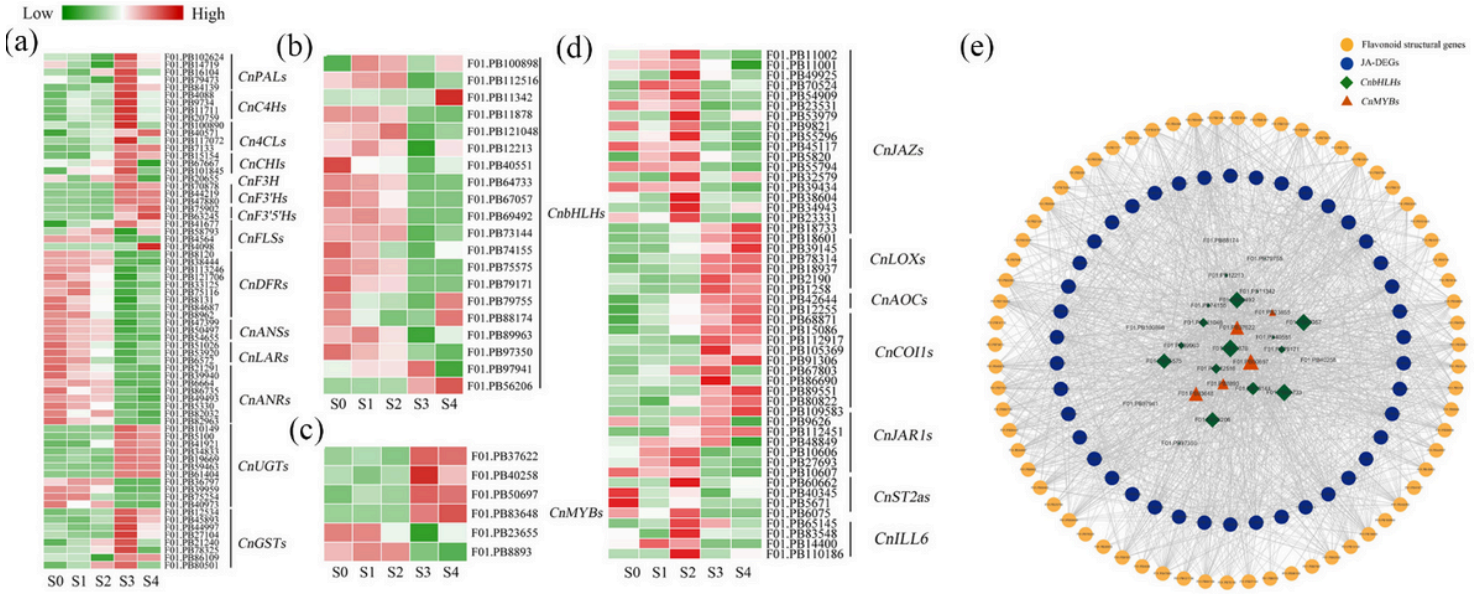

Figure 4

Heat maps and network correlation analysis. Heat maps of flavonoid (a), bHLH (b), MYB (c), and JA-related genes (d). (e) Network correlation analysis of *bHLHs*, *MYBs*, JA- and flavonoid-related genes.

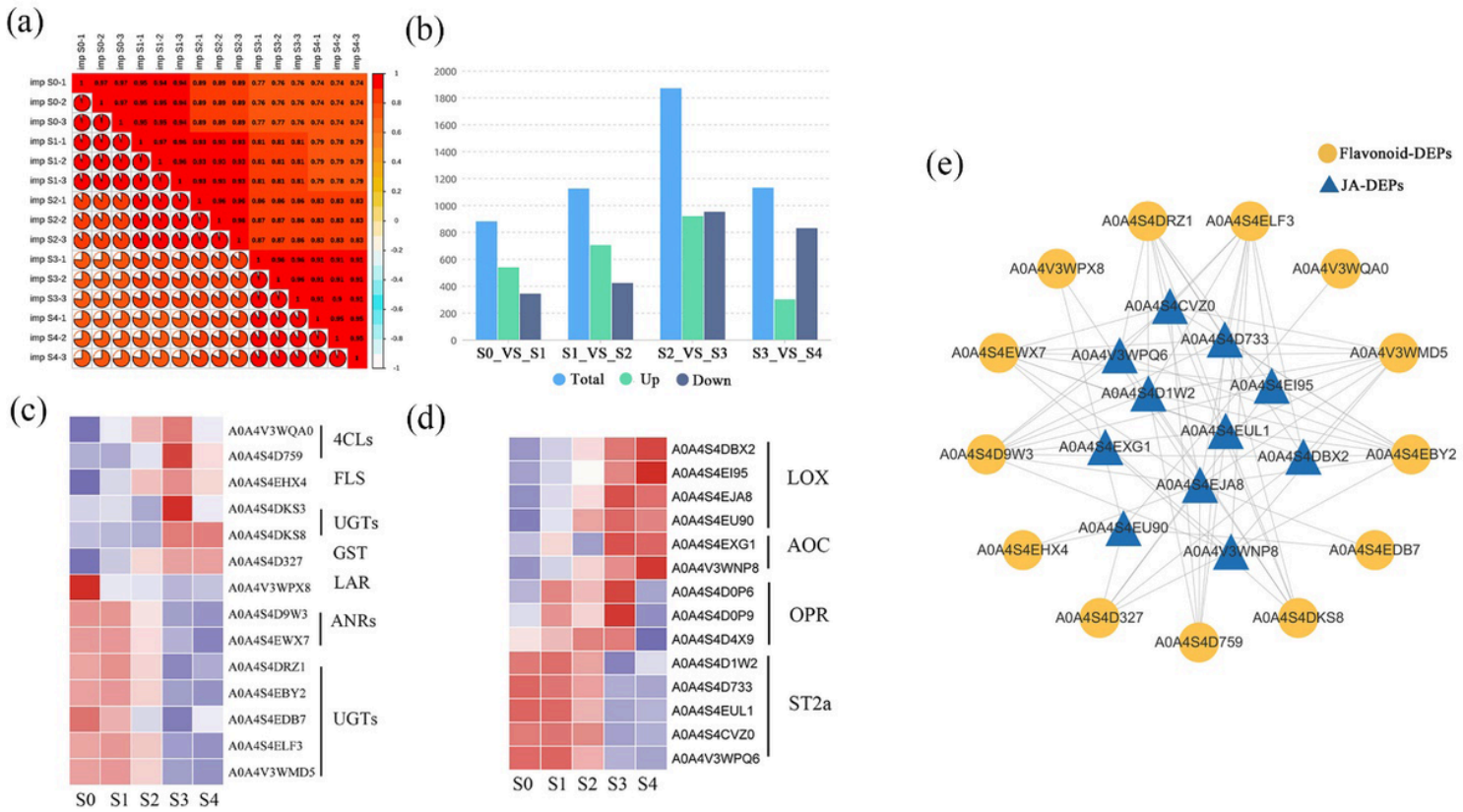

Figure 5

Analysis of proteome data. (a) Correlations of proteome data samples. (b) Histogram of distribution of differential proteins in each period. Heat maps of flavonoid (c), and JA-related genes (d). (e) Network correlation analysis of JA- and flavonoid-related proteins.

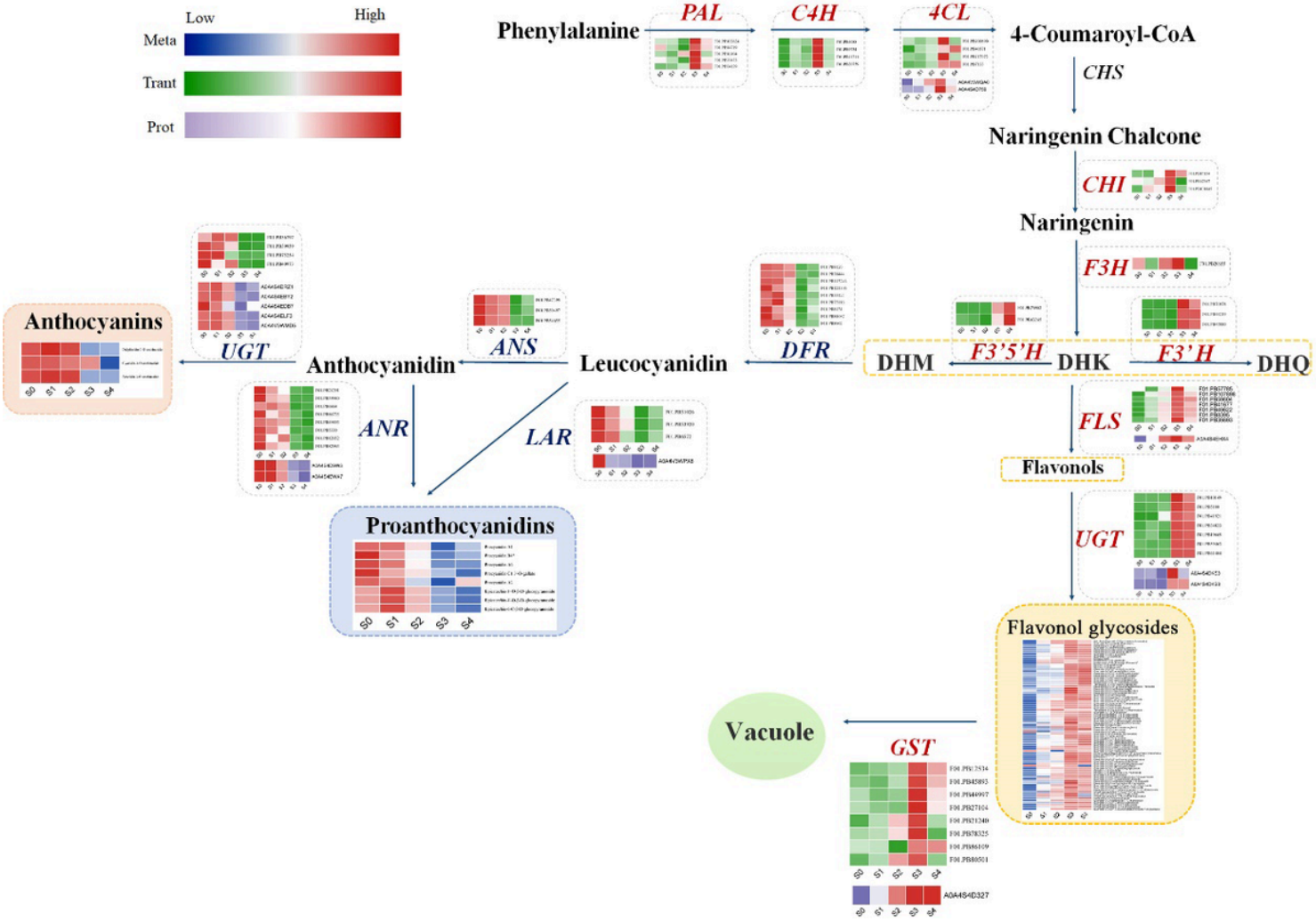

Figure 6

DEGs, DEPs and DEMs involved in the biosynthesis of the flavonoid pathway in *C. nitidissima*.

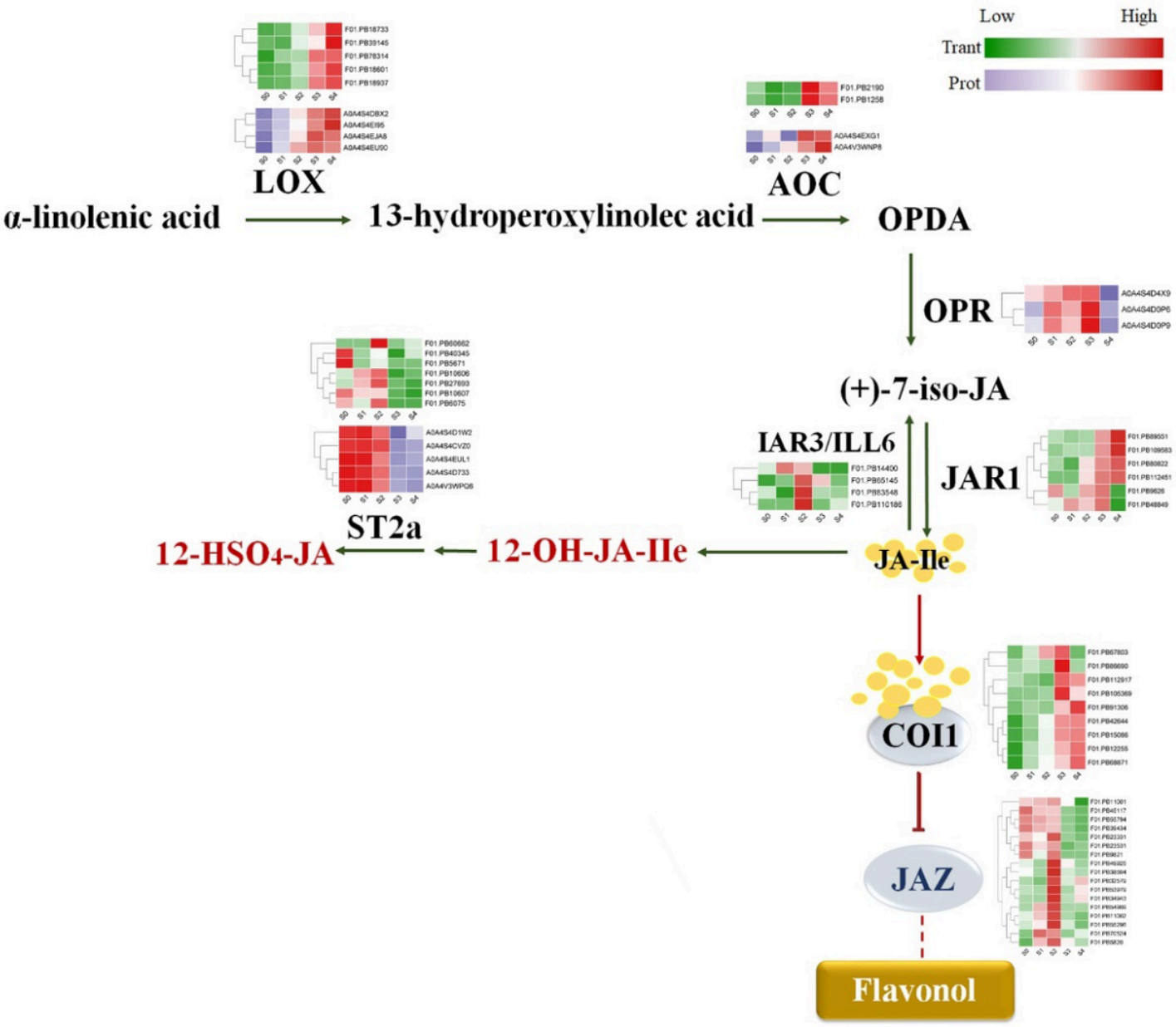

Figure 7

A model for the involvement of JA in the biosynthesis of flavonoids in *C. nitidissima*.

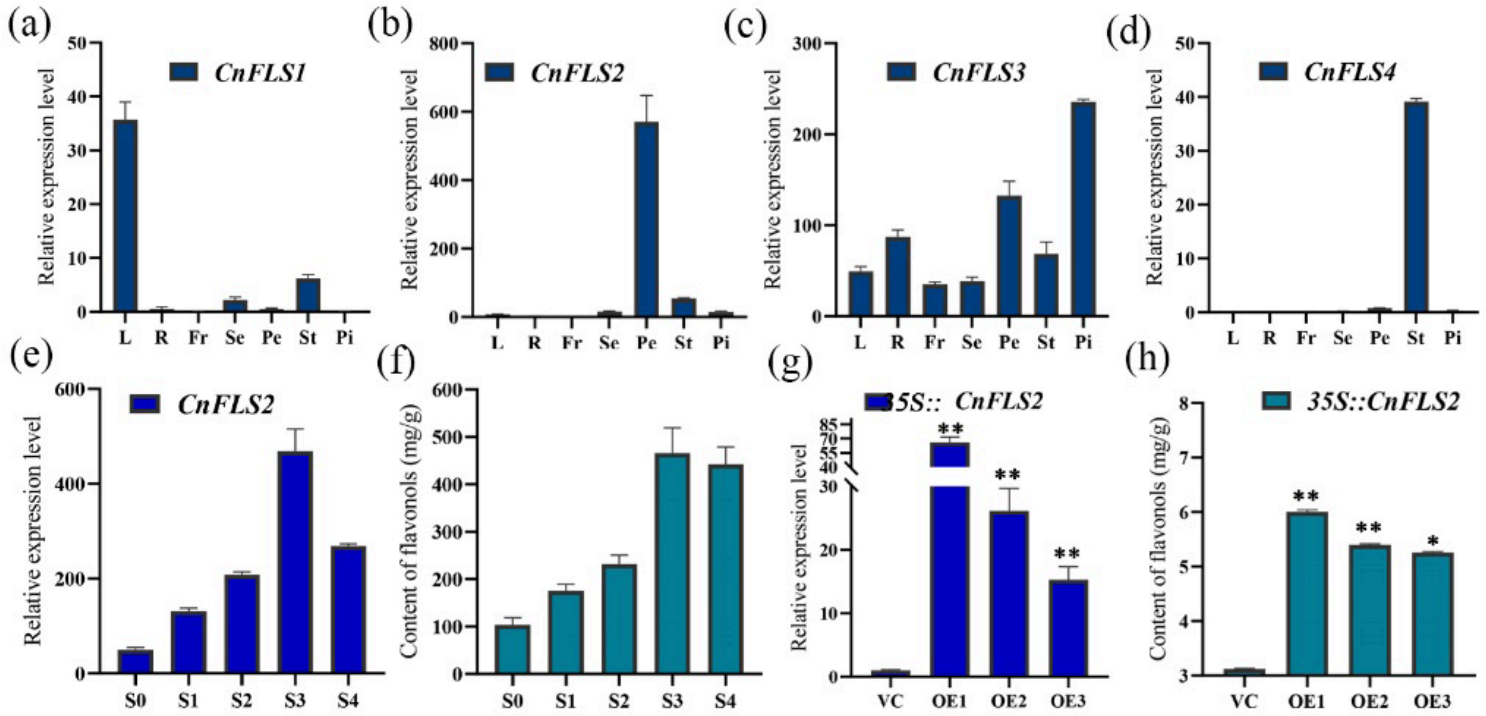

Figure 8

The expression analysis and transient overexpression of *CnFLS2*in *C. nitidissima*. Tissue-specific analysis of *CnFLS1* (a), *CnFLS2* (b), *CnFLS3* (c), *CnFLS4* (d); L means leaf, R means root, Fr means fruit, Se means sepal, Pe means petal, St means stamen, Pi means pistil. The expression of *CnFLS2* (e) and content of flavonol (f) at five developmental stages of petals. S0, early-bud stage; S1, mid-bud stage; S2, late-bud stage; S3, half-opening stage; S4, complete-opening stage. The expression of *CnFLS2* (g) and content of flavonol (h) analyses after transient overexpression treatment. VC, empty vector line; OE, overexpression line. Statistical significance was determined using Student's t-test (*P < 0.05, **P < 0.01).

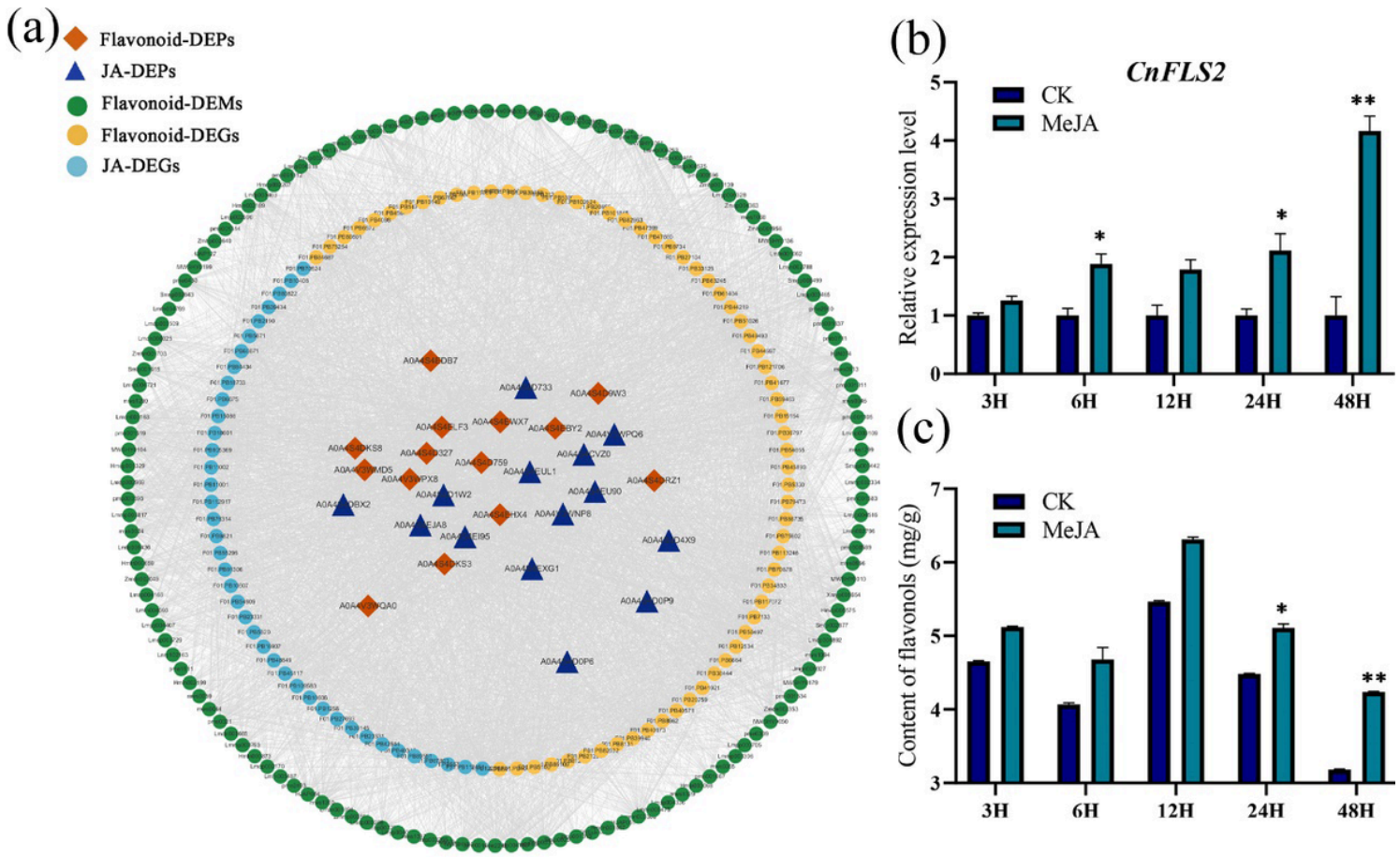

Figure 9

The conjoint analysis (a) of DEMs, DEGs, and DEPs, and expression of *CnFLS2* (b) and content of flavonol (c) after MeJA treatment.